MC-Stereo: Multi-Peak Lookup and Cascade Search Range for Stereo Matching

Miaojie Feng[1,*]   Junda Cheng[1,*]   Hao Jia[1]   Longliang Liu[1]   Gangwei Xu[1]

Qingyong Hu[2]   Xin Yang[1,†]

[1]School of EIC, Huazhong University of Science and Technology

[2]Academy of Military Sciences, Beijing, China

Abstract

Stereo matching is a fundamental task in scene comprehension. In recent years, the method based on iterative optimization has shown promise in stereo matching. However, the current iteration framework employs a single-peak lookup, which struggles to handle the multi-peak problem effectively. Additionally, the fixed search range used during the iteration process limits the final convergence effects. To address these issues, we present a novel iterative optimization architecture called MC-Stereo. This architecture mitigates the multi-peak distribution problem in matching through the multi-peak lookup strategy, and integrates the coarse-to-fine concept into the iterative framework via the cascade search range. Furthermore, given that feature representation learning is crucial for successful learn-based stereo matching, we introduce a pre-trained network to serve as the feature extractor, enhancing the front end of the stereo matching pipeline. Based on these improvements, MC-Stereo ranks first among all publicly available methods on the KITTI-2012 and KITTI-2015 benchmarks, and also achieves state-of-the-art performance on ETH3D. Code is available at https://github.com/MiaoJieF/MC-Stereo.

1. Introduction

Stereo matching is a crucial computer vision technology. Its primary objective is to establish the corresponding relationship between the identical scene or object in 3D space from two images. This technology finds widespread applications in various fields, including computer vision, robot navigation, augmented reality, virtual reality, and autonomous driving.

Traditional stereo matching methods [11, 28, 41] primarily depend on manually-crafted features and matching strategies, which exhibit suitability for simple scenes but may show limitations in handling complex scenes. The
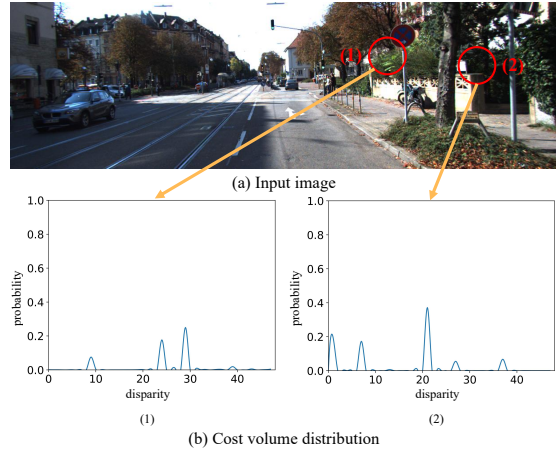

Figure 1. Illustration of multi-peak distribution in the cost volume. (a) Input left image. (b) The cost volume distribution of a single pixel in the center of the red circle.

deep learning-based stereo matching method [4, 10, 21, 31] improves the accuracy to a new height. Early deep learning-based stereo matching methods usually consist of 4 steps, including feature extraction, cost volume construction, cost aggregation, and disparity regression. These methods typically employ multi-layer 3D convolution for cost aggregation to regularize the cost volume. In recent years, the method [12, 30] based on iterative optimization has achieved milestone progress in optical flow estimation. Subsequently, RAFT-Stereo [15] introduces the framework of iterative optimization to stereo matching. Specifically, after constructing the cost volume, RAFT-Stereo [15] iteratively retrieves local costs through a GRU-based updater and regresses the disparity residual. This updater can preserve contextual information and previous states in hidden layers, and thus it can effectively combine context with local matching details and in turn progressively improve disparity estimation accuracy. However, there are two problems with the existing iteration framework [15, 32]. (1) We observe that the cost volume usually contains multi-peak distribution (as shown in Figure 1), and the existing iterative optimization based methods use single-peak lookup, which can not deal with the problem of multi-peak distribu-
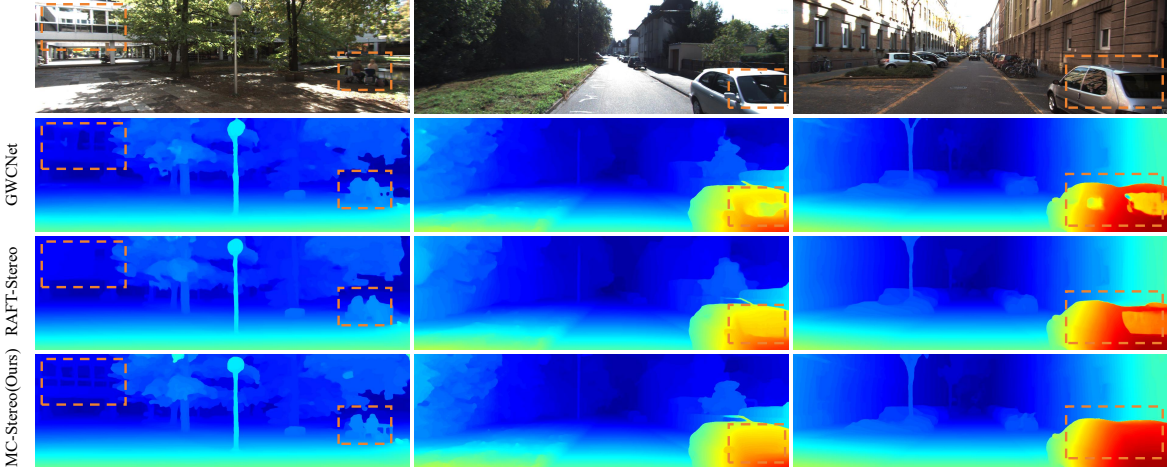
Figure 2. Qualitative results on KITTI. The second, third, and fourth rows are the results of GWCNet [10], RAFT-Stereo [15] and our MC-Stereo respectively. Our MC-Stereo performs better in reflective areas.

tion well. (2) The process of iterative optimization should be modeled as a process of gradual refinement. However, the existing framework method uses a single fixed search range, which limits its final convergence effect.

In this paper, we propose the multi-peak lookup strategy and cascade search range to solve these two problems. The purpose of multi-peak lookup strategy is to improve the ability of the model to handle multi-peak distribution. In each iteration, the multi-peak lookup strategy indexes several local cost volumes with high probability, then integrates information through GRU, and finally regresses the disparity. The cascade search range divides the iterative optimization process into multiple stages, using a specific search range at each stage. Specifically, we use a large search range at the beginning of iterative optimization and gradually reduce the search range according to a specific pattern. This design is based on the idea of coarse to fine, a large search range at the beginning is conducive to accelerating convergence, and a small search range at the end is conducive to finer results. Experiments show that the proposed method can effectively improve the performance. In addition, feature representation learning is the key to realizing learning-based stereo matching. However, in the field of stereo matching, feature extraction has not been improved significantly for many years. We introduce a network pre-trained on a large dataset as feature extractor to improve the front end deficiencies in pipeline. We name our method MC-Stereo. Based on these improvements, MC-Stereo ranks 1st among all publicly available methods on the KITTI-2012 [9] and KITTI-2015 [22] benchmarks, and also achieves state-of-the-art performance on ETH3D [24]. Our contribution can be summarized as follows:

- We propose the multi-peak lookup strategy to improve the ability of the model in dealing with multi-peak distribution.

- We propose a cascade search strategy, which combines the idea of coarse to fine into the iterative optimization framework.
- Our proposed MC-Stereo ranks 1st among all published methods on the KITTI-2012 and KITTI-2015 benchmarks, and also achieves SOTA performance on ETH3D.

2. Related Work

Traditional stereo matching [11, 28, 41] typically consists of four steps: matching cost calculation, cost aggregation, disparity calculation, and disparity refinement. With the development of deep learning, each step in the traditional method can be replaced by a deep neural network for performance improvement. Zbontar and Lecun [37] first propose to replace the manually designed explicit metric function with the implicit metric learned by the network for computing matching cost. Seki et al. [25] propose SGM-Net which learns penalty parameters for semi-global matching (SGM).

In recent years, end-to-end networks have become the mainstream of stereo matching. Mayer et al. [21] propose the first end-to-end disparity regression network Disp-Net which constructs a correlation volume based on CNN features and then aggregates the correlation volume using 2D convolutions. Finally, the disparity map is regressed from the aggregated volume. As the cost volume is the key affecting the final accuracy and efficiency of stereo matching, subsequent studies [5, 6, 10, 31, 34] mainly focus on cost volume construction and aggregation. In FastACV, Xu et al. [33] utilize a multi-peak strategy that selects the top-K disparities with the maximum probabilities to construct a sparse cost volume. Such a strategy can greatly reduce the computational cost without compromising accuracy ex-
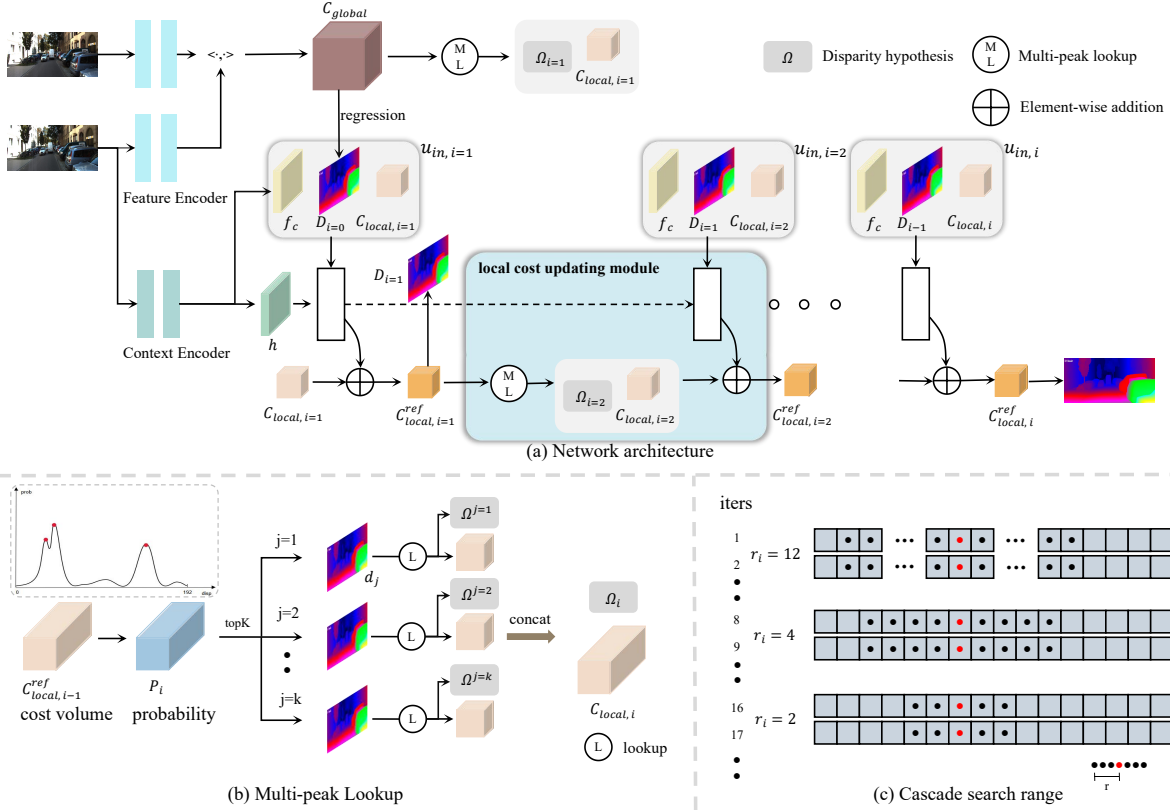
2

Figure 3. Overview of MC-Stereo. (a) The architecture of MC-Stereo consists of three main components: feature extraction, cost volume construction, and iterative optimization. The core of iterative optimization is the local cost updating module that is based on multi-peak lookup and cascade search range. (b) Multi-peak lookup. Since the cost volume contains multiple peaks, we uniformly sample around top K disparities with the largest probability from the probability volume as our disparity hypothesis. (c) Cascade search range. We divide the search range into N levels and set different search ranges according to the number of iterations.

cessively. Different from FastACV, in this work we not only select the top-K disparities but also uniformly samples around it to obtain more reliable distribution information. [36] and [20] explore depth distribution and sampling strategies on a cascade architecture, respectively. In comparison, our approach focuses on iterative optimization architecture and is much more concise.

Although various cost volumes have been developed, these cost volumes could inevitably contain redundancy and noises arising from matching errors and ambiguities at ill-posed regions (e.g., occluded regions, textureless/transparent regions, etc.). To alleviate these problems, several CNN based cost aggregation methods have been developed. For instance, GCNet [13] introduces 3D CNN based encoder-decoder to aggregate the cost volume. PSMNet [4], GWCNet [10] and ACVNet [31] adopt a stacked hourglass block with 3D convolutional layers for cost aggregation. However, processing cost volumes using 3D convolutions is usually computationally expensive which limits its application to high-resolution cost volumes. GANet [38] develops a semi-global aggregation layer and a locally

guided aggregation layer to replace 3D convolutions. However, such method increases the accuracy at the expense of the increased inference time. AANet [35] proposes an intra-scale and cross-scale cost aggregation algorithm to replace the traditional 3D convolution, which significantly improves the reasoning speed but leads to a decrease in accuracy. CoEx [1] introduces the Guided Cost volume Excitation (GCE) and demonstrates that the straightforward excitation of cost volume channels, guided by the image, can significantly enhance performance. Moreover, significant efforts [3, 17, 39, 40] have been directed towards enhancing the generalizability of stereo matching networks.

Recently, the recurrent iterative optimization framework (e.g., RAFT-Stereo [15]), which directly optimizes the disparity maps via recurrent GRU updaters, has achieved impressive performance. Subsequent work CREStereo [14] and IGEV-Stereo [32] continue this framework. But they all have two problems: (1) Using single-peak lookup is not conducive to dealing with multi-peak distribution. (2) Using a single fixed search range limits the final convergence accuracy. In this work, we propose the multi-peak lookup

strategy and cascade search range to address the above two issues.

3. Approach

3.1. Network Architecture

Figure 3 illustrates the architecture of our MC-Stereo which consists of three main modules: 1) feature extraction, 2) cost volume construction, and 3) iterative optimization.
Feature Extraction. We utilize two separate encoders, i.e., the *feature encoder* and the *context encoder*. For the *feature encoder*, we use the first two stages of the ConvNeXt [18] pretrained on ImageNet [8] to extract features for both the left and right images at 1/4 and 1/8 resolution. Then we fuse features of two different scales through a U-Net style up-sampling module to obtain the final feature maps with 1/4 resolution from the left image and right image respectively, denoted as $f_l, f_r \in R^{C \times H \times W}$, where C=256, H and W are 1/4 of original image width and height. We use the same network architecture as the *feature encoder* for the *context encoder*, with the only difference being that the *context encoder* is exclusively applied to the left image to obtain the context feature f_c and the initial hidden state h for the update operator.
Cost Volume Construction. We construct a correlation volume based on left and right feature maps $f_l, f_r \in R^{C \times H \times W}$ as:

$$C_{init}(d, x, y) = \langle f_l(x, y), f_r(x - d, y) \rangle \qquad (1)$$

where $\langle \cdot, \cdot \rangle$ is the inner product, d is the disparity $\in$ $[0, D_{max}/4]$, D_{max} is the maximum disparity hypothesis (192), (x,y) represents the pixel coordinates. And the constructed cost volume $C_{init} \in R^{D_{max}/4 \times H \times W}$ provides matching similarities between each pixel and all corresponding pixels in the right image with different disparities. Then, we apply average pooling along the disparity dimension of C_{init} using a kernel size of 1,2 and equivalent stride, resulting in a 2-layer cost volume pyramid $\{C^1, C^2\}$, which provides information of different receptive fields. For ease of description, we define the cost volume pyramid as C_{global}. When we perform a subsequent look-up operation on C_{global}, it actually retrieves each cost volume within the cost volume pyramid. During later iterative optimization, C_{global} is not updated.
Iterative Optimization. We convert C_{init} into a probability volume via the softmax operation along the disparity dimension. Next, we use multi-peak lookup to select the top K disparities with the largest probability from the probability volume which serves as the initial disparity index for local cost volume aggregation from C_{global}. The updater produces a residual that updates the local cost volume, from which the disparity is computed. The top K disparity hypotheses with the highest probability are selected

again from the updated local cost for the next iteration. We present details of iterative optimization with multi-peak lookup and cascade search range in Sec. 3.2-3.4.

3.2. Iterative Optimization

Preliminary: We obtain the final disparity by iterating the **local cost updating module**. In general, in the ith iteration, the input of the local cost updating module is the output of the updating module in previous iteration, i.e., the refined local cost $C_{local,i-1}^{ref}$ and the disparity map D_{i-1} in i-1 iteration. Naturally, the outputs of the current iteration are denoted as $C_{local,i}^{ref}$ and D_i.

local cost updating module. To be specific, for the ith iteration, we first take the refined local cost volume (denoted as $C_{local,i-1}^{ref}$) which is refined in the previous iteration i-1 as the input of the multi-peak lookup operation (denoted as ML) to determine the disparity hypotheses set of the current iteration (denoted as Ω_i) and construct the current local cost $C_{local,i}$ as Equation 2, the details are explained in Sec. 3.3. Then we utilize GRUs for updating the local cost volume. We concatenate the current iteration local cost $C_{local,i}$, previous iteration disparity map D_{i-1} and the context feature f_c as the input of GRUs (denoted as $u_{in,i}$) to obtain the residual of the local cost, denoted as $\triangle C_{local,i}$. $\triangle C_{local,i}$ is added with the current iteration local cost volume to obtain the refined local cost volume $C_{local,i}^{ref}$ as follow:

$$\Omega_i, C_{local,i} = ML(C_{local,i-1}^{ref}) \qquad (2)$$

$$\Delta C_{local,i} = GRU(u_{in,i}) \qquad (3)$$

$$C_{local,i}^{ref} = C_{local,i} + \Delta C_{local,i} \qquad (4)$$

We transform the refined local cost volume $C_{local,i}^{ref}$ into a probability distribution by the softmax operation. The current iteration disparity map D_i can be obtained as:

$$D_i = \sum_{m \in \Omega_i} m \cdot \text{softmax}\left(C_{local,i}^{ref}\right) \qquad (5)$$

In special cases, the first iteration, i.e., i=1, the input of the local updating module is from C_{global} as shown in Figure 3.

3.3. Multi-Peak Lookup

One of the most important steps in recurrent optimization is to index the local cost volume from C_{global}. This lookup operation is represented by L_C in RAFT-Stereo [15]. In the previous approach, only one single disparity obtained from the previous iteration is used to index the local cost volume. However, we believe that such single-peak search strategy may be inadequate when dealing with multi-peak distribution. For disparity probabilities with a multi-peak distribution, the single-peak lookup strategy fails to sample

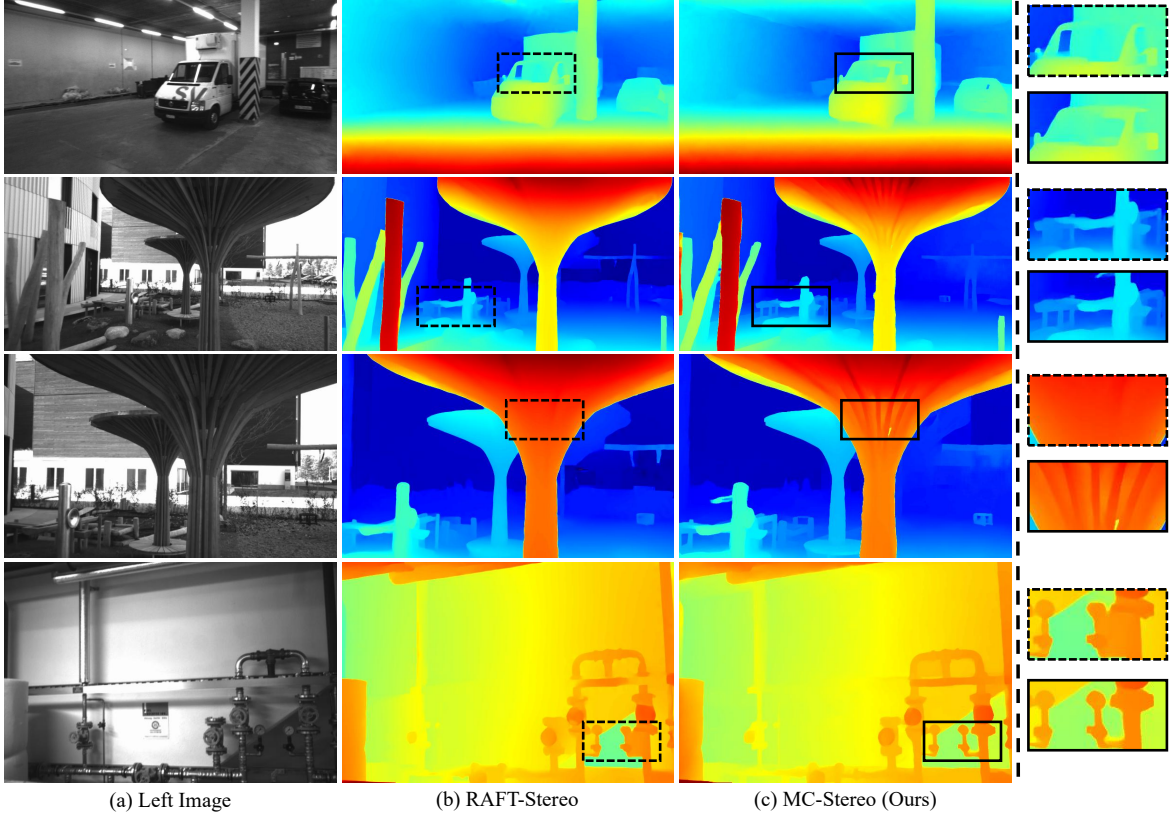| (a) Left Image | (b) RAFT-Stereo | (c) MC-Stereo (Ours) |

Figure 4. Qualitative results on ETH3D. The second and third columns are the results of RAFT-Stereo [15] and our MC-Stereo respectively.

the local cost volume in the appropriate range, resulting in the final disparity estimation falling into a wrong peak. To solve this problem, we propose the multi-peak lookup strategy.

The process of multi-peak lookup is shown in Figure 3 (b). To be specific, we first transform the previous iteration refined local cost volume $C_{local,i-1}^{ref}$ into a probability distribution P_i through softmax, and the dimension of P_i is $[N_{i-1}, H/4, W/4]$, where N_{i-1} is the number of sampling points in the i-1 iteration. In each iterations, $N_{i-1} = k \times (2r_{i-1} + 1)$, where k is the peak number of multi-peak look up, and r_{i-1} is the search radius of the i-1 iteration. After obtaining the probability distribution, we obtain the k disparity values d_j $(j = 1, \ldots, k)$ with the largest probabilities. For each disparity d_j, we uniformly sample around d_j in the range of -r and +r to obtain the subset of the disparity hypotheses, denoted as Ω^j, then merge all subsets together to obtain the final current iteration disparity hypotheses Ω_i as follow:

$$\Omega^j = [d_j - r_i, \ldots, d_j, \ldots, d_j + r_i], (j = 1, \ldots, k) \quad (6)$$

$$\Omega_i = [\Omega^1, \Omega^2, \ldots, \Omega^k] \quad (7)$$

And we construct the current iteration local cost volume $C_{local,i}$ by indexing from the C_{global} according to the depth hypotheses Ω_i.

3.4. Cascade Search Range

The search range $(2 \times r_i + 1)$ refers to the range of the grid for indexing from the global cost volume. The size of the search range affects the convergence speed and accuracy. The previous approaches use the same search range in all iterations, which could result in imprecision. At the beginning of recurrent optimization, applying a large search range can accelerate convergence and avoid falling into local optimum. In the later stage of optimization, a smaller search range can eliminate some disturbing items to improve matching accuracy. Based on this observation, we propose the cascade search range to further improve the matching accuracy. Our method searches with different ranges on the same resolution. Specifically, as shown in Figure 3 (c), we divide the search range into three levels, i.e., 25, 9, and 5. Each level corresponds to particular GRU updaters. In the first few iterations, we use a large search range, and then reduce the search range step by step as follows:

$$r_i = \begin{cases} 12, & i = 1, \ldots, 6 \\ 4, & i = 7, \ldots, 16 \\ 2, & i = 17, \ldots, 32 \end{cases} \quad (8)$$

5

Method	All				Ref		Time
	2-noc	2-all	3-noc	3-all	2-noc	3-noc	(s)
PSMNet [4]	2.44	3.01	1.49	1.89	13.77	8.36	0.31
GwcNet [10]	2.16	2.71	1.32	1.70	12.49	7.80	0.20
HITNet [29]	2.00	2.65	1.41	1.89	9.75	5.91	0.02
CFNet [26]	1.90	2.43	1.23	1.58	9.91	5.96	0.18
LEAStereo [7]	1.90	2.39	1.13	1.45	9.66	5.35	0.30
ACVNet [31]	1.83	2.35	1.13	1.47	11.42	7.03	0.20
LaC+GANet [16]	1.72	2.26	<u>1.05</u>	1.42	10.40	6.02	1.60
PCWNet [27]	<u>1.69</u>	2.18	**1.04**	<u>1.37</u>	8.94	4.99	0.44
IGEV-Stereo [32]	1.71	<u>2.17</u>	1.12	1.43	<u>7.29</u>	<u>4.11</u>	0.32
CREStereo [14]	1.72	2.18	1.14	1.46	9.71	6.27	0.41
MC-Stereo(Ours)	**1.55**	**1.99**	**1.04**	**1.34**	**6.82**	**4.10**	0.40

Table 1. **Quantitative evaluation KITTI-2012 [9] benchmark.** Percentages of erroneous pixels for both non-occluded (noc) and all pixels are reported. 'All' denotes all pixels of the image, and 'Ref' denotes pixels of reflective area. Bold: Best, Underscore: Second best. The inference time is measured on a single NVIDIA RTX 3090 GPU at KITTI resolution (376×1248).

3.5. Loss Function

We use the L1 loss between the predicted and ground truth disparity for a sequence of N refinement predictions of disparity, $\{d_1, \ldots, d_N\}$. Given ground truth d_{gt}, the loss is defined as:

$$L_{stereo} = \sum_{i=1}^{N} \gamma^{N-i} \|d_{gt} - d_i\| \qquad (9)$$

where $\gamma = 0.9$.

4. Experiments

This section details the experimental results of our proposed model on multiple datasets. We evaluate MC-Stereo on KITTI-2012 [9], KITTI-2015 [22], ETH3D [24], and Scene Flow [21]. Our method achieves state-of-the-art performance on the KITTI-2012, KITTI-2015, and ETH3D leaderboards.

4.1. Implementation details

We implement MC-Stereo in PyTorch [23] and use an AdamW [19] optimizer. And all experiments are performed on two NVIDIA RTX 3090 GPUs. We uniformly set the number of iterations to 32 when testing on KITTI-2012 [9], KITTI-2015 [22], ETH3D [24] leaderboard. Data augmentation is used including saturation change, image perturbance, and random scales. Following previous work, we pretrain our model on Scene Flow [21] training set for 200k steps with a batch size of 8. For the KITTI-2012 and KITTI-2015 leaderboards, we finetune the pre-trained Scene Flow model on the mixed KITTI-2012 and KITTI-2015 training set. For ETH3D, we finetune the pre-trained Scene Flow model on the mixed CREStereo Dataset [14], InStereo2K [2] and ETH3D [24] dataset.

4.2. MC-Stereo Performance

4.2.1 KITTI-2012

We submit MC-Stereo to the KITTI-2012 [9] stereo benchmark. Among all published methods on the KITTI-2012 leaderboard, MC-Stereo ranks 1st on several evaluation metrics. Details are shown in Table 1. On Out-Noc under 2 pixels error threshold, our MC-Stereo outperforms the next best method PCWNet [27] by 8.28%. On Out-All under 2 pixels error threshold, our MC-Stereo surpasses the second best method IGEV-Stereo [32] by 8.29%. On Out-Noc under 2 pixels error threshold in reflective area, our MC-Stereo outperforms the next best method IGEV-Stereo [32] by 6.44%.

4.2.2 KITTI-2015

At the time of writing this paper, our MC-Stereo ranks 1st on the KITTI-2015 [22] leaderboard among all published methods (See Table 2). On the percentage of erroneous foreground pixels, our MC-Stereo outperforms RAFT-Stereo [15] and IGEV-Stereo [32] by 13.15% and 5.99%. Figure 2 shows qualitative results on KITTI. Our MC-Stereo performs better in reflective areas.

4.2.3 ETH3D

Table 3 summarizes the results on the ETH3D [24] leaderboard. MC-Stereo achieves state-of-the-art performance on ETH3D. At the time of writing this paper, MC-Stereo ranks 1st on the 50% error quantile. Figure 4 shows qualitative results on ETH3D.

Method	All			Noc			Time
	D1-bg	D1-fg	D1-all	D1-bg	D1-fg	D1-all	(s)
PSMNet [4]	1.86	4.62	2.32	1.71	4.31	2.14	0.31
GwcNet [10]	1.74	3.93	2.11	1.61	3.49	1.92	0.20
HITNet [29]	1.74	3.2	1.98	1.54	2.72	1.74	0.02
CFNet [26]	1.54	3.56	1.88	1.43	3.25	1.73	0.18
LEAStereo [7]	1.40	2.91	1.65	1.29	2.65	1.51	0.30
ACVNet [31]	<u>1.37</u>	3.07	1.65	<u>1.26</u>	2.84	1.52	0.20
LaC+GANet [16]	1.44	2.83	1.67	<u>1.26</u>	2.64	<u>1.49</u>	1.60
PCWNet [27]	<u>1.37</u>	3.16	1.67	<u>1.26</u>	2.93	1.53	0.44
RAFT-Stereo [15]	1.75	2.89	1.91	-	-	-	0.38
IGEV-Stereo [32]	1.38	<u>2.67</u>	<u>1.59</u>	1.27	2.62	1.49	0.32
CREStereo [14]	1.45	2.86	1.69	1.33	<u>2.60</u>	1.54	0.41
MC-Stereo(Ours)	**1.36**	**2.51**	**1.55**	**1.24**	**2.55**	**1.46**	0.40

Table 2. **Quantitative evaluation KITTI-2015 [22] benchmark.** Percentages of disparity outliers D1 for background, foreground, and all pixels are reported. 'All' denotes all pixels of the image, and 'Noc' denotes the non-occluded pixels. Bold: Best, Underscore: Second best.

Method	bad 4.0(%)	AvgErr	50% error quantile
HITNet [29]	0.19	0.20	0.10
GwcNet [10]	0.50	0.35	0.20
CFNet [26]	0.56	0.27	0.15
ACVNet [31]	0.20	0.23	0.15
RAFT-Stereo [15]	0.15	0.18	0.10
CREStereo [14]	**0.10**	**0.13**	<u>0.09</u>
IGEV-Stereo [32]	<u>0.11</u>	<u>0.14</u>	<u>0.09</u>
MC-Stereo(Ours)	**0.10**	<u>0.14</u>	**0.08**

Table 3. **Quantitative evaluation on ETH3D [24] benchmark.** Fraction of pixels with errors larger than 4 (bad 4.0), the per-pixel average disparity error, and 50% error quantile on non-occluded area are reported. Bold: Best, Underscore: Second best.

4.2.4 Scene Flow

On Scene Flow [21] test set, MC-Stereo achieves competitive results. Details results are summarized in Table 4. Visual comparisons are shown in Figure 5. Our MC-Stereo effectively captures intricate details in objects that have fine structures.

4.3. Ablation Study

A series of ablation studies are conducted to verify the effectiveness of each component in MC-Stereo. All ablation experiments are trained on the Scene Flow [21] dataset for 200k iterations with a batch size of 8.

Cascade Search Range: We conduct a comprehensive ablation experiment on the cascade search range, and the results are summarized in Table 5. The search radius of '4' is commonly employed in existing iterative optimization

Method	Scene Flow		
	EPE	>1px(%)	>3px(%)
PSMNet [4]	1.07	10.90	4.40
GwcNet [10]	0.79	8.19	3.40
ACV-Net [31]	0.48	-	-
LEAStereo [7]	0.78	7.82	-
RAFT-Stereo [15]	0.60	6.77	3.18
IGEV-Stereo [32]	<u>0.47</u>	<u>5.21</u>	<u>2.48</u>
MC-Stereo(Ours)	**0.45**	**4.97**	**2.32**

Table 4. **Quantitative evaluation on Scene Flow [21] test set.** Percentages of erroneous pixels and average end-point errors are reported. Bold: Best, Underscore: Second best.

frameworks. With a total of 32 iterations, we divide the iterative optimization process into three stages. Initially, we expand the search radius in the first stage to conduct the experiment, subsequently narrowing the search range in the third stage based on this initial analysis. The results indicate that the cascade search range, based on the coarse-to-fine approach, outperforms a single fixed search range.

Multi-Peak Lookup: Table 6 presents the results of the ablation experiment on multi-peak lookup. The label 'No' signifies the utilization of the single-peak lookup strategy, while the variable 'K' represents the number of peaks set in the multi-peak lookup approach. The findings demonstrate a consistent performance improvement between multi-peak and single-peak lookup strategies. Moreover, as K approaches 3, the benefits gained from employing the multi-peak lookup strategy tend to plateau.

Pretrained Feature Extractor: Accurate feature representation learning is crucial for successful learn-based stereo matching. In Table 7, we compare the performance of a fea-

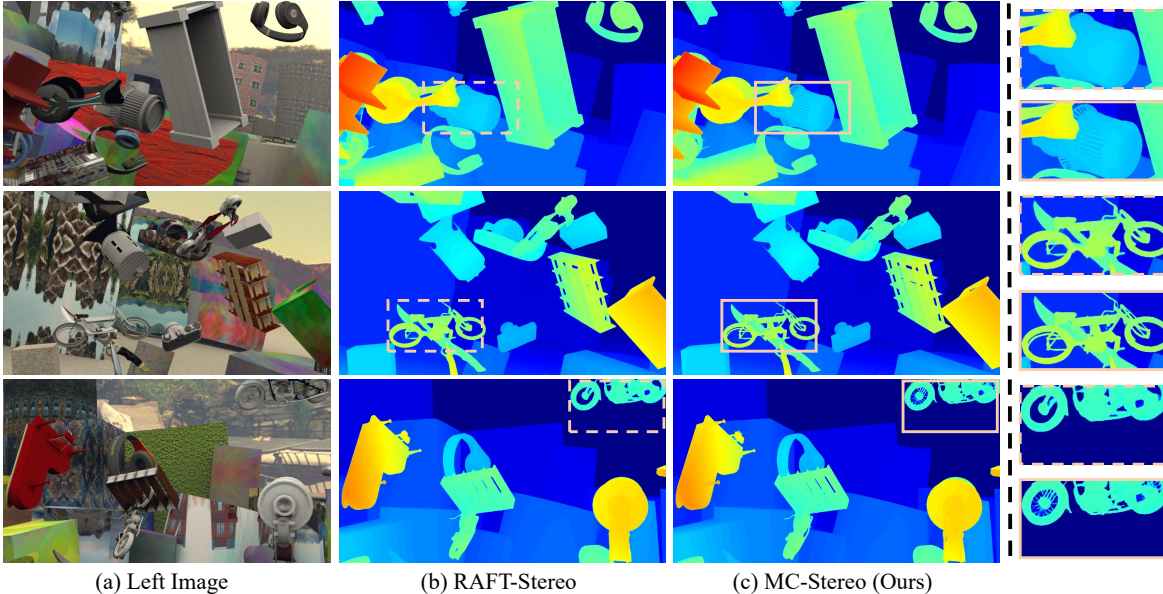| | (a) Left Image | (b) RAFT-Stereo | (c) MC-Stereo (Ours) |

Figure 5. Qualitative results on Scene Flow. The second and third columns are the results of RAFT-Stereo [15] and our MC-Stereo respectively. Our MC-Stereo effectively captures intricate details in objects that have fine structures.

	Iter	Iter	Iter	Scene Flow		
	1~6	7~16	17~32	EPE	>1px(%)	>3px(%)
Search Radius	4	4	4	0.53	5.96	2.73
	12	4	4	0.51	5.80	2.63
	12	4	2	0.50	5.74	2.62

Table 5. **Ablation study of cascade search range.**

ture extraction network initialized with random parameters to one loaded with pre-trained parameters on ImageNet [8]. The results demonstrate that pre-training on ImageNet enhances the characterization ability of the extracted features, thereby benefiting stereo matching. It is worth noting that pre-training on ImageNet is primarily intended for classifying tasks. However, the dissimilarities between matching tasks may restrict the complete benefits of pre-training. Exploring dedicated pre-training methods for matching tasks is a worthwhile endeavor for future research.

5. Limitation

Our multi-peak lookup strategy and cascade search range achieve significant performance improvements, but the hyperparameters (such as the number of peaks for multi-peak lookup, series division, search range, etc.) are set empirically. When dealing with new scenarios, these parameters may need to be readjusted for best performance. In future work, we will focus on making hyperparameter settings dynamic, allowing the network to choose independently according to the scenario.

Variations		Scene Flow			Param
		EPE	>1px(%)	>3px(%)	(M)
Multi-peak Lookup	No	0.50	5.74	2.62	21.2M
	K=2	0.49	5.43	2.56	21.3M
	K=3	0.48	5.38	2.55	21.4M
	K=4	0.48	5.37	2.55	21.5M

Table 6. **Ablation study of multi-peak lookup.** Settings used in our final model are underlined.

Experiment	Variations	Scene Flow		
		EPE	>1px(%)	>3px(%)
Pretrained		0.48	5.38	2.55
Feature Extractor	√	0.45	4.97	2.32

Table 7. **Ablation study of feature extractor.**

6. Conclusion

We have proposed MC-Stereo, a new learning based method for Stereo Matching. The multi-peak lookup strategy improves the ability of the model to deal with multi-peak distribution. Cascade search range combines the idea of coarse to fine into the iterative optimization framework. Our method ranks first among all published methods on the KITTI-2012 and KITTI-2015 leaderboards, and also achieves state-of-the-art performance on the ETH3D benchmark.

References

[1] Antyanta Bangunharcana, Jae Won Cho, Seokju Lee, In So Kweon, Kyung-Soo Kim, and Soohyun Kim. Correlate-and-excite: Real-time stereo matching via guided cost volume excitation. In *2021 IEEE/RSJ International Conference on Intelligent Robots and Systems (IROS)*, pages 3542–3548. IEEE, 2021. 3

[2] Wei Bao, Wei Wang, Yuhua Xu, Yulan Guo, Siyu Hong, and Xiaohu Zhang. Instereo2k: a large real dataset for stereo matching in indoor scenes. *Science China Information Sciences*, 63:1–11, 2020. 6

[3] Changjiang Cai, Matteo Poggi, Stefano Mattoccia, and Philippos Mordohai. Matching-space stereo networks for cross-domain generalization. In *2020 International Conference on 3D Vision (3DV)*, pages 364–373. IEEE, 2020. 3

[4] Jia-Ren Chang and Yong-Sheng Chen. Pyramid stereo matching network. In *Proceedings of the IEEE conference on computer vision and pattern recognition*, pages 5410–5418, 2018. 1, 3, 6, 7

[5] Junda Cheng, Xin Yang, Yuechuan Pu, and Peng Guo. Region separable stereo matching. *IEEE Transactions on Multimedia*, 2022. 2

[6] Junda Cheng, Gangwei Xu, Peng Guo, and Xin Yang. Coatrsnet: Fully exploiting convolution and attention for stereo matching by region separation. *International Journal of Computer Vision*, pages 1–18, 2023. 2

[7] Xuelian Cheng, Yiran Zhong, Mehrtash Harandi, Yuchao Dai, Xiaojun Chang, Hongdong Li, Tom Drummond, and Zongyuan Ge. Hierarchical neural architecture search for deep stereo matching. *Advances in Neural Information Processing Systems*, 33:22158–22169, 2020. 6, 7

[8] Jia Deng, Wei Dong, Richard Socher, Li-Jia Li, Kai Li, and Li Fei-Fei. Imagenet: A large-scale hierarchical image database. In *2009 IEEE conference on computer vision and pattern recognition*, pages 248–255. Ieee, 2009. 4, 8

[9] Andreas Geiger, Philip Lenz, and Raquel Urtasun. Are we ready for autonomous driving? the kitti vision benchmark suite. In *2012 IEEE conference on computer vision and pattern recognition*, pages 3354–3361. IEEE, 2012. 2, 6

[10] Xiaoyang Guo, Kai Yang, Wukui Yang, Xiaogang Wang, and Hongsheng Li. Group-wise correlation stereo network. In *Proceedings of the IEEE/CVF Conference on Computer Vision and Pattern Recognition*, pages 3273–3282, 2019. 1, 2, 3, 6, 7

[11] Heiko Hirschmuller. Stereo processing by semiglobal matching and mutual information. *IEEE Transactions on pattern analysis and machine intelligence*, 30(2):328–341, 2007. 1, 2

[12] Shihao Jiang, Dylan Campbell, Yao Lu, Hongdong Li, and Richard Hartley. Learning to estimate hidden motions with global motion aggregation. In *Proceedings of the IEEE/CVF International Conference on Computer Vision*, pages 9772–9781, 2021. 1

[13] Alex Kendall, Hayk Martirosyan, Saumitro Dasgupta, Peter Henry, Ryan Kennedy, Abraham Bachrach, and Adam Bry. End-to-end learning of geometry and context for deep stereo

[14] Jiankun Li, Peisen Wang, Pengfei Xiong, Tao Cai, Ziwei Yan, Lei Yang, Jiangyu Liu, Haoqiang Fan, and Shuaicheng Liu. Practical stereo matching via cascaded recurrent network with adaptive correlation. In *Proceedings of the IEEE/CVF Conference on Computer Vision and Pattern Recognition*, pages 16263–16272, 2022. 3, 6, 7

[15] Lahav Lipson, Zachary Teed, and Jia Deng. Raft-stereo: Multilevel recurrent field transforms for stereo matching. In *2021 International Conference on 3D Vision (3DV)*, pages 218–227. IEEE, 2021. 1, 2, 3, 4, 5, 6, 7, 8

[16] Biyang Liu, Huimin Yu, and Yangqi Long. Local similarity pattern and cost self-reassembling for deep stereo matching networks. In *Proceedings of the AAAI Conference on Artificial Intelligence*, pages 1647–1655, 2022. 6, 7

[17] Biyang Liu, Huimin Yu, and Guodong Qi. Graftnet: Towards domain generalized stereo matching with a broad-spectrum and task-oriented feature. In *Proceedings of the IEEE/CVF Conference on Computer Vision and Pattern Recognition*, pages 13012–13021, 2022. 3

[18] Zhuang Liu, Hanzi Mao, Chao-Yuan Wu, Christoph Feichtenhofer, Trevor Darrell, and Saining Xie. A convnet for the 2020s. In *Proceedings of the IEEE/CVF Conference on Computer Vision and Pattern Recognition*, pages 11976–11986, 2022. 4

[19] Ilya Loshchilov and Frank Hutter. Decoupled weight decay regularization. *arXiv preprint arXiv:1711.05101*, 2017. 6

[20] Yamin Mao, Zhihua Liu, Weiming Li, Yuchao Dai, Qiang Wang, Yun-Tae Kim, and Hong-Seok Lee. Uasnet: Uncertainty adaptive sampling network for deep stereo matching. In *Proceedings of the IEEE/CVF International Conference on Computer Vision*, pages 6311–6319, 2021. 3

[21] Nikolaus Mayer, Eddy Ilg, Philip Hausser, Philipp Fischer, Daniel Cremers, Alexey Dosovitskiy, and Thomas Brox. A large dataset to train convolutional networks for disparity, optical flow, and scene flow estimation. In *Proceedings of the IEEE conference on computer vision and pattern recognition*, pages 4040–4048, 2016. 1, 2, 6, 7

[22] Moritz Menze, Christian Heipke, and Andreas Geiger. Joint 3d estimation of vehicles and scene flow. *ISPRS annals of the photogrammetry, remote sensing and spatial information sciences*, 2:427, 2015. 2, 6, 7

[23] Adam Paszke, Sam Gross, Francisco Massa, Adam Lerer, James Bradbury, Gregory Chanan, Trevor Killeen, Zeming Lin, Natalia Gimelshein, Luca Antiga, et al. Pytorch: An imperative style, high-performance deep learning library. *Advances in neural information processing systems*, 32, 2019. 6

[24] Thomas Schops, Johannes L Schonberger, Silvano Galliani, Torsten Sattler, Konrad Schindler, Marc Pollefeys, and Andreas Geiger. A multi-view stereo benchmark with high-resolution images and multi-camera videos. In *Proceedings of the IEEE conference on computer vision and pattern recognition*, pages 3260–3269, 2017. 2, 6, 7

[25] Akihito Seki and Marc Pollefeys. Sgm-nets: Semi-global matching with neural networks. In *Proceedings of the*

regression. In *Proceedings of the IEEE international conference on computer vision*, pages 66–75, 2017. 3

IEEE conference on computer vision and pattern recognition, pages 231–240, 2017. 2

[26] Zhelun Shen, Yuchao Dai, and Zhibo Rao. Cfnet: Cascade and fused cost volume for robust stereo matching. In *Proceedings of the IEEE/CVF Conference on Computer Vision and Pattern Recognition*, pages 13906–13915, 2021. 6, 7

[27] Zhelun Shen, Yuchao Dai, Xibin Song, Zhibo Rao, Dingfu Zhou, and Liangjun Zhang. Pcw-net: Pyramid combination and warping cost volume for stereo matching. In *Computer Vision–ECCV 2022: 17th European Conference, Tel Aviv, Israel, October 23–27, 2022, Proceedings, Part XXXII*, pages 280–297. Springer, 2022. 6, 7

[28] Jian Sun, Nan-Ning Zheng, and Heung-Yeung Shum. Stereo matching using belief propagation. *IEEE Transactions on pattern analysis and machine intelligence*, 25(7):787–800, 2003. 1, 2

[29] Vladimir Tankovich, Christian Hane, Yinda Zhang, Adarsh Kowdle, Sean Fanello, and Sofien Bouaziz. Hitnet: Hierarchical iterative tile refinement network for real-time stereo matching. In *Proceedings of the IEEE/CVF Conference on Computer Vision and Pattern Recognition*, pages 14362–14372, 2021. 6, 7

[30] Zachary Teed and Jia Deng. Raft: Recurrent all-pairs field transforms for optical flow. In *European conference on computer vision*, pages 402–419. Springer, 2020. 1

[31] Gangwei Xu, Junda Cheng, Peng Guo, and Xin Yang. Attention concatenation volume for accurate and efficient stereo matching. In *Proceedings of the IEEE/CVF Conference on Computer Vision and Pattern Recognition*, pages 12981–12990, 2022. 1, 2, 3, 6, 7

[32] Gangwei Xu, Xianqi Wang, Xiaohuan Ding, and Xin Yang. Iterative geometry encoding volume for stereo matching. In *Proceedings of the IEEE/CVF Conference on Computer Vision and Pattern Recognition*, pages 21919–21928, 2023. 1, 3, 6, 7

[33] Gangwei Xu, Yun Wang, Junda Cheng, Jinhui Tang, and Xin Yang. Accurate and efficient stereo matching via attention concatenation volume. *IEEE Transactions on Pattern Analysis and Machine Intelligence*, 2023. 2

[34] Gangwei Xu, Huan Zhou, and Xin Yang. Cgi-stereo: Accurate and real-time stereo matching via context and geometry interaction. *arXiv preprint arXiv:2301.02789*, 2023. 2

[35] Haofei Xu and Juyong Zhang. Aanet: Adaptive aggregation network for efficient stereo matching. In *Proceedings of the IEEE/CVF Conference on Computer Vision and Pattern Recognition*, pages 1959–1968, 2020. 3

[36] Jiayu Yang, Jose M Alvarez, and Miaomiao Liu. Non-parametric depth distribution modelling based depth inference for multi-view stereo. In *Proceedings of the IEEE/CVF Conference on Computer Vision and Pattern Recognition*, pages 8626–8634, 2022. 3

[37] Jure Zbontar, Yann LeCun, et al. Stereo matching by training a convolutional neural network to compare image patches. *J. Mach. Learn. Res.*, 17(1):2287–2318, 2016. 2

[38] Feihu Zhang, Victor Prisacariu, Ruigang Yang, and Philip HS Torr. Ga-net: Guided aggregation net for end-to-end stereo matching. In *Proceedings of the IEEE/CVF Con-ference on Computer Vision and Pattern Recognition*, pages 185–194, 2019. 3

[39] Feihu Zhang, Xiaojuan Qi, Ruigang Yang, Victor Prisacariu, Benjamin Wah, and Philip Torr. Domain-invariant stereo matching networks. In *Computer Vision–ECCV 2020: 16th European Conference, Glasgow, UK, August 23–28, 2020, Proceedings, Part II 16*, pages 420–439. Springer, 2020. 3

[40] Jiawei Zhang, Xiang Wang, Xiao Bai, Chen Wang, Lei Huang, Yimin Chen, Lin Gu, Jun Zhou, Tatsuya Harada, and Edwin R Hancock. Revisiting domain generalized stereo matching networks from a feature consistency perspective. In *Proceedings of the IEEE/CVF Conference on Computer Vision and Pattern Recognition*, pages 13001–13011, 2022. 3

[41] Ke Zhang, Jiangbo Lu, and Gauthier Lafruit. Cross-based local stereo matching using orthogonal integral images. *IEEE transactions on circuits and systems for video technology*, 19 (7):1073–1079, 2009. 1, 2